Molecular basis for the control of motor-based transport of MHC class II compartments

Rocha, N.

Chapter 4

A splice variant of RILP induces lysosomal clustering independent of dynein recruitment

Reproduced from Biochem Biophys Res Commun.2006.344:747-56

A splice variant of RILP induces lysosomal clustering independent of dynein recruitment

Marije Marsman [1], Ingrid Jordens [1], Nuno Rocha, Coenraad Kuijl, Lennert Janssen, Jacques Neefjes *

Division of Tumor Biology, The Netherlands Cancer Institute, Amsterdam 1066CX, The Netherlands

Received 14 March 2006
Available online 6 April 2006

Abstract

The small GTPase Rab7 controls fusion and transport of late endocytic compartments. A critical mediator is the Rab7 effector RILP that recruits the minus-end dynein–dynactin motor complex to these compartments. We identified a natural occurring splice variant of RILP (RILPsv) lacking only 27 amino acids encoded by exon VII. Both variants bind Rab7, prolong its GTP-bound state, and induce clustering of late endocytic compartments. However, RILPsv does not recruit the dynein–dynactin complex, implicating exon VII in motor recruitment. Clustering might still occur via dimerization, since both RILP and RILPsv are able to form hetero- and homodimers. Moreover, both effectors compete for Rab7 binding but with different outcome for dynein–dynactin recruitment and transport. Hence, RILPsv provides an extra dimension to the control of vesicle fusion and transport by the small GTPase Rab7.

Keywords: Rab7; RILP; Late endosomes; Lysosomes; Dynein; MTOC

Compartments of the biosynthetic and endocytic pathways continuously undergo fusion and fission events to maintain their integrity. The family of Rab GTPases regulates these processes. Beside regulating membrane fusion, Rab GTPases also regulate membrane transport [1–4]. In principle, one single Rab can regulate distinct steps in these processes by binding to one or more effector proteins. Moreover, each Rab member localizes to a specific compartment and cycles between an active GTP-bound state and an inactive GDP-bound state, thereby providing a temporal and spatial resolution in the regulation of membrane transport and fusion, for review see [4–8].

Rab7 is a key regulator in transport and fusion of late endosomes and lysosomes [9–14]. Three Rab7 effectors have been described, Rab7-interacting lysosomal protein (RILP), oxysterol-binding protein (OSBP)-related protein-1L (ORP1L), and Rabring7 [1,15–17]. Rabring7 has a zinc finger domain and specifically interacts with Rab7-GTP. Expression of Rabring7 results in clustering of late endosomes and lysosomes in the perinuclear area [16]. ORP1L expression can also induce lysosomal clustering. ORP1L has a conserved OSBP-related ligand-binding domain, an N-terminal extension with three ankyrin repeats, and a pleckstrin homology domain (PHD). RILP, which is unrelated to ORP1L and Rabring7, also interacts with Rab7-GTP and overexpression induces clustering of late endosomes and lysosomes [1,15]. In addition, both RILP and ORP1L can induce recruitment of the motor complex dynein–dynactin onto late endosomes and lysosomes, which facilitates their transport towards the minus-end of the microtubules [1,17].

Recently, the Golgi-restricted Rab34 has been implicated in lysosomal positioning [18]. Overexpression of wild type or constitutively active Rab34 resulted in clustering of late endosomal and lysosomal compartments in the perinuclear area. Although the precise mechanism has not

* Corresponding author. Fax: +31 02 5122029.
E-mail address: j.neefjes@nki.nl (J. Neefjes).
[1] These authors contributed equally to this work.

been revealed, it could be due to interaction with RILP [18].

Two RILP-like proteins have been identified, RLP1 and RLP2 [19], which share two highly conserved RILP homology domains, RH1 and RH2. Interestingly, both RLP1 and RLP2 are unable to bind to Rab7 and cannot induce lysosomal clustering. Yet, insertion of a domain of RILP (aa 274–333), containing the recently identified Rab7-binding domain, causes RLP1 to interact with Rab7 and to induce clustering of late endosomes and lysosomes [20].

Here, we describe a splice variant of RILP (RILPsv) lacking exon VII (aa 315–342). RILPsv still interacts with Rab7-GTP, but it lacks the ability to induce recruitment of the dynein–dynactin complex. However, like RILP, RILPsv can dimerize and is able to induce clustering of Rab7-positive compartments. Co-expression of full-length RILP can restore motor recruitment in RILPsv-expressing cells indicating that RILP can compete with RILPsv for Rab7 binding in vivo. Thus, splice variants can add an additional layer of complexity to regulation of intracellular vesicle transport.

Materials and methods

Plasmids. Wild type Rab7 [11,21] and Rab5 [22,23] were subcloned into the bacterial expression vectors pRP261 to generate glutathione-*S*-transferase (GST) fusion proteins. For myc-tagging Rab7 was cloned into pcDNA3. For yeast two-hybrid assay, the Rab7 binding half of RILP and RILPsv were both cloned into pACT. Rab7wt, Rab7Q67L, Rab7T22N, and Rab7I125N were after deletion of the CAAX box cloned into the pGBT9 (Stratagene). GFP-Rab7wt, GFP-RILPdeltaN (aa 199–401), and RILP-myc were described before [1].

RILPsv was subcloned into eukaryotic expression vector pcDNA3 (Invitrogen) with or without myc-tag introduced by PCR. All PCR products were sequence verified. For GFP-tagging both RILP and RILPsv were subcloned into the eukaryotic EGFP-C1 vector (Clontech).

RT-PCR. Human tissue RNAs were obtained from D. Atsma (Pathology, Netherlands Cancer Institute) isolated from lung, lymph node, and intestine. RNAs were isolated from the cell lines T47D (breast carcinoma), 603D (melanoma), and WiDR, and Colo205 (colon carcinoma) by TriZol following the manufacturer's protocol. mRNAs transcribed using SuperScript™ II reverse transcriptase (Invitrogen) by oligo(dT). The first-strand cDNA synthesis was performed using oligo's QS (654–673 bp) and QAS3 (1218–1238 bp). This product was used in a second nested PCR using WTS (751–768 bp) and QAS3.

Antibodies and markers. The following antibodies were used: rabbit polyclonal anti-CD63 [24] and mouse monoclonal anti-CD63 (Cymbus Biotechnology), mouse monoclonal anti-EEA-1 (BD Transduction laboratories), mouse monoclonal anti-Golgin-97 (Molecular Probes), mouse monoclonal anti-dynactin p50 and mouse monoclonal anti-p150^{Glued} (BD Transduction laboratories), mouse monoclonal anti-vsv (P5D4F7) and mouse monoclonal anti-myc (9E10), and rabbit polyclonal anti-RILP [1]. For immuno-staining, antibodies were diluted in PBS containing 0.5% BSA. Alexa 488- or Texas Red/Alexa 568-conjugated mouse or rabbit secondary antibodies were used (Molecular Probes, Leiden, The Netherlands).

For living cell analyses, lysosomal compartments were labeled by LysoTracker Red (Molecular Probes, Leiden).

Tissue culture. The human melanoma cell line Mel JuSo was maintained in Iscoves medium (GIBCO-BRL) supplemented with 7.5% FCS, 2 mM glutamine, 100 U/ml penicillin, and 100 μg/ml streptomycin. Mel JuSo stably transfected with GFP-Rab7 [1] were maintained in the same medium supplemented with 500 μg/ml G418 (GIBCO-BRL). The cells were grown at 37 °C under 5% CO_2. HeLa cells were maintained in Iscoves medium (GIBCO-BRL) supplemented with 7.5% FCS, 2 mM glutamine, 100 U/ml penicillin, and 100 μg/ml streptomycin. Cells were transiently transfected by polyethylenimine 25 kDa (PEI) transfection (Polysciences). The transfectants were cultured for 24–48 h prior to fixation or further processing.

Micro-injection and confocal analyses. For micro-injection, cells were seeded on coverslips in medium lacking G418 24 h before the experiment, to achieve 40–60% confluency at the time of injection. Cells were injected on a heated xy stage of an Olympus XL70 microscope equipped with an Eppendorf manipulator 5171/transjector 5246 system. Usually, 50–100 cells were injected intranuclearly with a mix of cDNAs (100–200 ng/μl). Texas Red Dextran-70 (Molecular Probes, Leiden) was used as injection marker. Cells were subsequently cultured at 37 °C and, 3–7 h after micro-injection, living cells were analyzed or cells were fixed and immuno-stained before analysis. Fixation was either in 3.7% formaldehyde for 15 min followed by permeabilization in 0.1% Triton X-100 or in methanol (−20 °C) for 2 min. All experiments presented were repeated several times on different days and results were consistent and reproducible.

Confocal analyses were performed using a Leica TCS SP confocal laser-scanning microscope (CLSM) equipped with an Argon/Krypton laser (Leica Microsystems, Heidelberg, Germany). Green fluorescence was detected at $\lambda > 515$ nm after excitation at $\lambda = 488$ nm. For dual analyses, green fluorescence was detected at $\lambda = 520$–560 nm. Red fluorochromes were excited at $\lambda = 568$ nm and detected at $\lambda > 585$ nm.

Fluorescence recovery after photobleaching. Fluorescence recovery after photobleaching (FRAP) experiments were performed as described [1,25]. In brief, Mel JuSo cells expressing GFP-Rab7 were grown on coverslips in Iscoves medium lacking G418 at least 48 h before the experiment. cDNA encoding RILP or RILPsv mixed with 70 kDa TxR-dextran were introduced by micro-injected and cells were analyzed in culture chamber at 37 °C by CLSM. A small set of fluorescent vesicles was bleached for 1 s by a high intensity laser beam and the fluorescence recovery in the bleached spot was quantified. LysoTracker Red was used to identify the bleached vesicles. When RILP or RILPsv was introduced, FRAP analysis was performed 1–4 h after micro-injection in cells where clustering of the Rab7-positive vesicles was apparent. The experiments were performed on multiple cells and at various days. Because the bleached vesicles were not completely stationary their positions were tracked by LysoTracker Red and corrected with a program written in Matlab (Mathworks).

Expression and purification of recombinant proteins. RILP and RILPsv were expressed in *Escherichia coli* strain Rosetta(DE3)pLysS (Novagen) at 20 °C overnight as hexahistidine-tagged (His_6-tagged) fusions using the pETM-11 expression vector (kind gift of Gunther Stier, EMBL, Heidelberg, Germany). After collection, bacteria were resuspended in buffer A (25 mM Hepes, pH 7.5, 300 mM NaCl, complete EDTA-free tablets (Roche), 1 mM PMSF, 5 mM β-mercaptoethanol, 10 mM imidazole, and 0.05% (v/v) Triton X-100) and lysed by sonication on ice. All subsequent steps were performed at 4 °C. Lysates were loaded onto pre-equilibrated BD Talon Metal Affinity (Clontech) resin and washed with buffer A containing 20 mM imidazole. The resin was then packed into a column and bound proteins were eluted with buffer A containing 400 mM imidazole. Eluted proteins were concentrated in storage buffer (25 mM Hepes, pH 7.5, 300 mM NaCl, and 10% (v/v) glycerol) using a Vivaspin-2 concentrator (Vivascience), shock-frozen, and stored at −80 °C.

Rab7 was cloned into pET-28a (Novagen) and expressed as His_6-tag fusion in *E. coli* strain BL21(DE3)pLysS. Recombinant His-Rab7 protein was purified under native conditions by affinity-chromatography using Ni^{2+} according to the manufacturers (Qiagen).

Rab7 and Rab5 were expressed in Rosetta(DE3)pLysS as GST fusions using the expression vector pRP261, a derivative of pGEX-3X (Amersham Biosciences). GST-fusions were affinity-purified using the glutathione–Sepharose 4B resin (Amersham Biosciences) as described by the manufacturer. Protein concentration was determined using the Bradford protein concentration assay (Bio-Rad) calibrated with bovine serum albumin standards.

Pull-down assays and immunoblot analysis. For the GST pull-down assay, 100 μg of GTPγS preloaded GST-Rab7 or GST-Rab5 immobilized on 20 μl of packed glutathione–Sepharose 4B (Amersham Biosciences)

resin was used per 5×10^6 Mel JuSo cells. For the His-tag pull-down assay, 20 µg of either His_6-RILP or His_6-RILPsv was immobilized on 10 µl of packed Talon resin.

Mel Juso cells were electroporated with either GFP-RILP or GFP-RILPsv. At 24–30 h after electroporation, cells were washed twice with PBS and lysed for 20 min on ice in binding buffer (20 mM Hepes, pH 7.5, 100 mM NaCl, 0.1% (v/v) Nonidet P-40, 5 mM EDTA, 10 mM $MgCl_2$, 1 mM DTT, and Complete EDTA-free protease inhibitor cocktail (Roche)). Total lysates were cleared by centrifugation at 12,000*g* for 10 min at 4 °C. Supernatants were incubated with immobilized GST-fusions or His_6-fusions for 2 h at 4 °C. Resin fractions were washed five times with 20 mM Hepes, pH 7.5, 150 mM NaCl, 0.1% (v/v) Nonidet P-40, 10 mM $MgCl_2$, and 1 mM DTT and resuspended in reducing Laemmli sample buffer. Protein samples were separated by SDS–PAGE, transferred onto PVDF membranes and probed with polyclonal anti-GFP before detection by ECL (Amersham).

In vitro GTPase assay. GTPase activity in solution was assayed by release of [^{32}P]Pi using a modified charcoal binding assay [26,27]. His_6-Rab7 (50 pmol) was preloaded with 4 µl of [γ-^{32}P]GTP (5000 Ci/mmol, Amersham Biosciences) in preload buffer (50 mM Tris/HCl, pH 7.5, 250 mM NaCl, 1 mM DTT, 5% (v/v) glycerol, and 0.5 mg/ml BSA) supplemented with 10 mM EDTA on ice for 2 h in 10 µl total volume. Preload reactions were diluted with 20 µl of preload buffer supplemented with 20 mM $MgCl_2$ prior to passage at 4 °C through a P-6 polyacrylamide Micro Bio-Spin column (Bio-Rad) pre-equilibrated with preload buffer supplemented with 10 mM $MgCl_2$.

The effect of RILP or RILPsv on the intrinsic GTP hydrolysis of Rab7 was analyzed by incubating preloaded His_6-Rab7 in reaction buffer (40 mM Tris/HCl, pH 8.0, 8 mM $MgCl_2$, 1 mM DTT, and 2 mM GTP) alone (intrinsic hydrolysis) or with 3 µM of His_6-RILP, His_6-RILPsv, or BSA. Reactions were performed for 5 h at 25 °C. Triplicate timed 50 µl aliquots were mixed with 1 ml of 7% activated charcoal (w/v) in 10 mM KH_2PO_4 on ice. The mixture was vortexted, and centrifuged at 3000*g* for 5 min at 4 °C, and the [^{32}P]Pi release in the pellet fraction was quantified by liquid scintillation counting.

Results

RILPsv, a natural occurring splice variant of the Rab7 effector RILP

Late endosomal and lysosomal transport is regulated by the small GTPase Rab7 and its effector RILP (Rab7-interacting lysosomal protein) [1,15]. Upon activation, Rab7 interacts with RILP, thereby recruiting the minus-end motor complex dynein–dynactin, which results in the accumulation of late endosomal/lysosomal compartments at the microtubule-organizing center (MTOC) [1].

Beside RILP, an alternatively spliced variant of RILP (RILPsv) was identified in the original yeast two-hybrid screen with Rab7. This variant lacks amino acids 315–342, encoded by exon VII, which represents a proline-rich region (Fig. 1A). RILPsv still contains the two coiled-coil regions and the spliced region partially overlaps with the area interacting with Rab7 and regulating clustering of late endosomes and lysosomes [19,20]. In the two-hybrid screen, the splice variant still interacted with Rab7, yet the preference for the GTP-bound form seemed less pronounced (Table S1).

Several human est sequences for RILP were found in the database that specifically lacks exon VII (data not shown). Moreover, RILPsv appeared to be present in different cell types and tissues, which is shown by RT-PCR (Fig. 1B). Two products corresponding to the expected sizes for, respectively, RILP and RILPsv appeared in the nested PCR using oligo's located in exon VI and VIII (Fig. 1B). As a positive control cDNA encoding RILP was used.

Ectopic expression of RILPsv causes clustering of late endocytic compartments

RILP induces clustering of late endosomal and lysosomal compartments tightly around the MTOC [1,15]. To compare the phenotypes of RILPsv and RILP, both proteins were expressed in Mel JuSo cells. Cells were fixed and stained for RILP (Fig. 2A, middle panels) and RILPsv (Fig. 2B, middle panels). The early endosomes and Golgi apparatus were identified by the markers EEA-1 (Figs. 2A and B, lower-left panel) and Golgin (Figs. 2A and B,

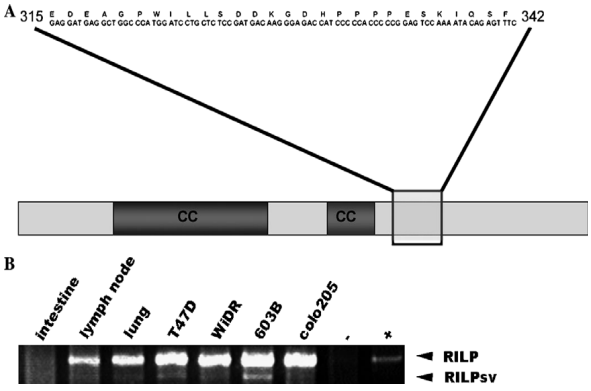

Fig. 1. A natural occurring splice variant of the Rab7 effector RILP. (A) Schematic representation of RILP (CC: represents the predicted coiled-coil region) and the amino acid sequence corresponding to exon VII, aa 315–342, absent in RILPsv is depicted by the gray box. (B) RNA isolated from indicated tissues and cell lines were analyzed by RT-PCR. PCR was performed with oligo's flanking exon VII and product sizes of both RILP and RILPsv are indicated.

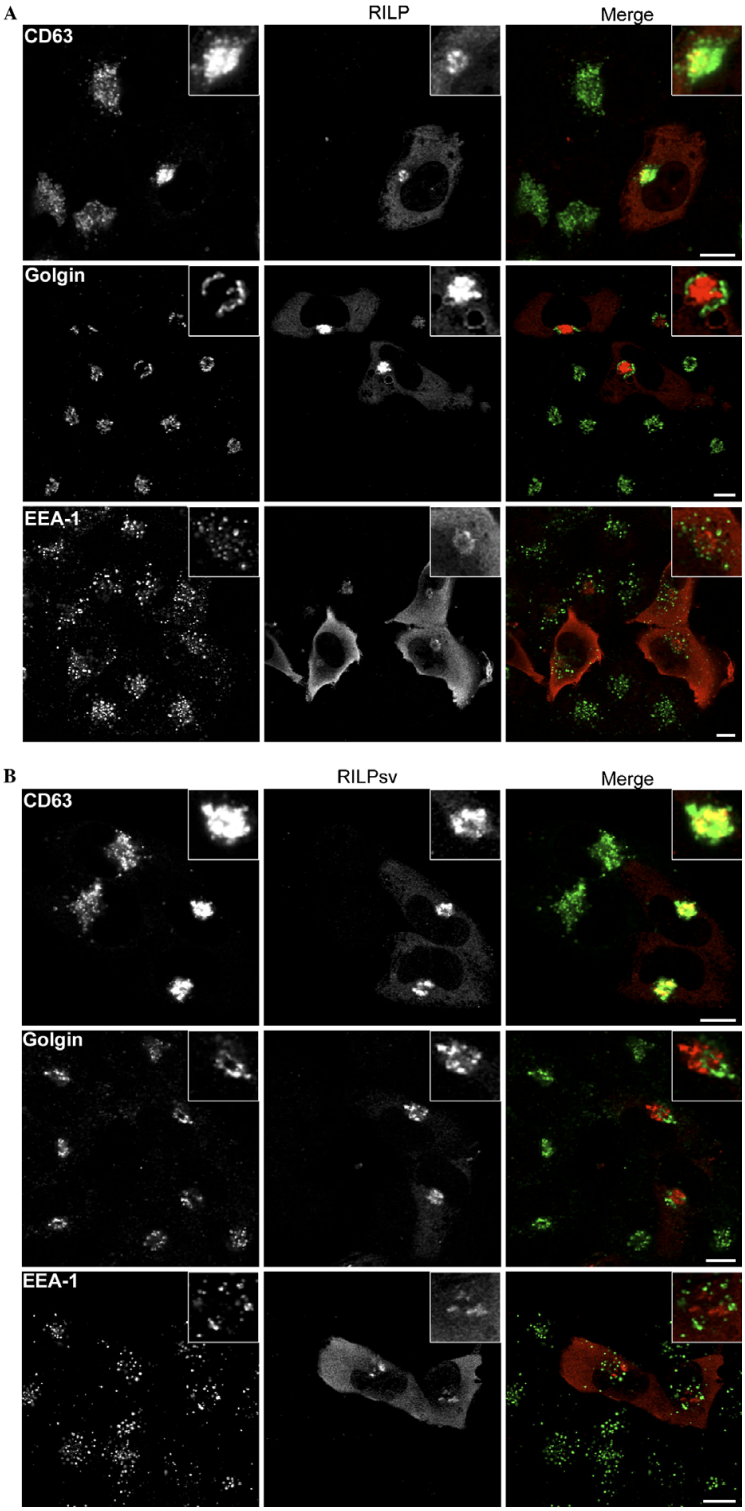
A
RILP
Merge
CD63
Golgin
EEA-1
B
RILPsv
Merge
CD63
Golgin
EEA-1

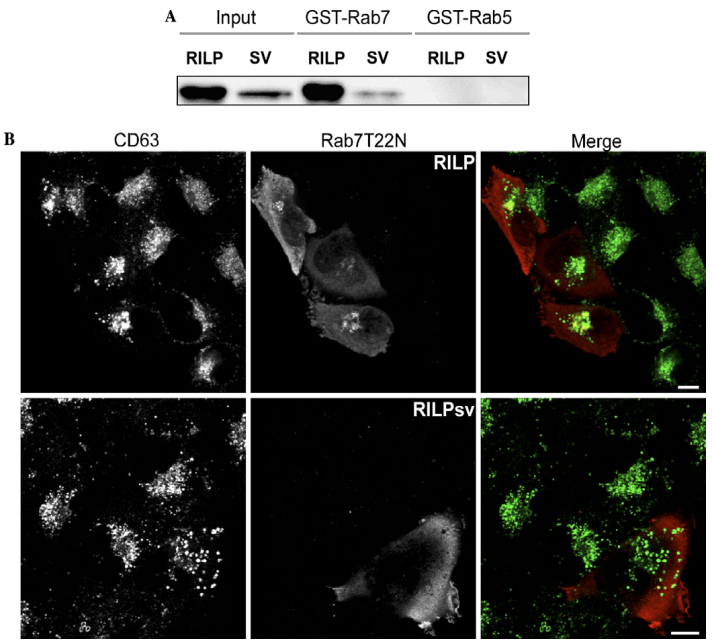

Fig. 3. Functional Rab7 is required for late endocytic clustering induced by RILPsv. (A) Equal amounts of GST-Rab7 or GST-Rab5 coupled to glutathione–Sepharose beads were incubated with cell lysates from Mel Juso cells expressing GFP-RILP or GFP-RILPsv. Proteins were transferred to PVDF and visualized by anti-GFP. RILP and RILPsv bind to GST-Rab7 (lanes 3 and 4), but not to GST-Rab5 (lanes 5 and 6). (B) Dominant-negative Rab7T22N was co-expressed in molar excess with RILP (upper panels) or RILPsv (lower panels) via micro-injection and immuno-labeled for CD63 (left panel) and RILP/RILPsv (middle panels). Co-expression of Rab7T22N (expression verified in single labeling; not shown) partially reversed the phenotypes of RILP and RILPsv (lower panels), shown by dispersed instead of clustered lysosomes (right panel). Bars equal 10 μm.

middle-left panel). RILPsv as well as RILP only affected the distribution of late endosomal and lysosomal compartments marked by CD63 (Figs. 2A and B, upper-left panel). The early endosomes were unaffected. It should be noted that the Golgi was still located perinuclearly, only the position of the late endosomes and lysosomes relative to the Golgi was affected. Whereas late endosomes and lysosomes in RILP-expressing cells moved inside the Golgi area, they remained clustered around or in-between the Golgi in RILPsv-expressing cells.

When the clusters were analyzed in more detail, we observed that the effect of RILP and RILPsv on late endosomal/lysosomal positioning was different. Whereas RILP induced a tight cluster of late endosomal/lysosomal compartments (Fig. 2A), RILPsv induced a less condensed, more dispersed cluster and often smaller separated clusters are observed (Fig. 2B). In HeLa cells, where late endosomes and lysosomes have a more dispersed localization, the difference between RILP and RILPsv is even more apparent (Figs. S1 and S2). These results indicate that exon VII affects clustering of late endosomes and lysosomes.

Functional Rab7 is necessary for late endosomal/lysosomal clustering induced by RILPsv

Both RILPsv and RILP interact with Rab7 in yeast two-hybrid assay. However, RILP induced a stronger transactivation, suggesting that it associates with Rab7 with a higher affinity (Table S1). To biochemically confirm that Rab7 interacts with both, RILP and RILPsv, Mel JuSo cells were transfected with cDNA encoding either EGFP-tagged RILP or RILPsv. Twenty-four hours after transfection, cells were lysed. Lysates were incubated with GST-Rab5wt or GST-Rab7wt immobilized on glutathione beads and

Fig. 2. RILPsv causes clustering of late endocytic compartments. (A) CLSM analyses of Mel Juso cells expressing either RILP or (B) RILPsv, immunolabeled with anti-CD63 (upper panel), anti-Golgin (middle panel) or anti-EEA-1 (lower panel). Both RILP and RILPsv only affect the localization of late endosomes and lysosomes as observed by clustering of CD63-positive compartments. Both EEA-1 and Golgi distribution are not affected, although the Golgi is partially repositioned when late endosomes and lysosomes occupy the space around the MTOC. Insets of the RILP clusters are shown in the upper right corner of the panel. Bars equal 10 μm.

bound proteins were detected by Western blotting with anti-GFP. Both EGFP-RILP and EGFP-RILPsv were pulled down only with GST-Rab7 and not with the related GST-Rab5 (Fig. 3A).

The involvement of Rab7 in the formation of the lysosomal clustering induced by RILPsv was studied in more detail by co-expression of a dominant-negative mutant of Rab7, Rab7T22N. High expression of Rab7T22N results in dispersion of the late endosomes and lysosomes. Upon co-expression with RILP, Rab7T22N can partially reverse RILP-induced clustering [1]. Cells were fixed and stained for CD63 (Fig. 3B, left panels), RILP or RILPsv (Fig. 3B, middle panels) 7 h after co-injection of cDNAs encoding, respectively, RILP or RILPsv and Rab7T22N. Clustering was reversed in a low percentage of the RILP-expressing cells, whereas almost all RILPsv-expressing cells showed a dispersed phenotype (Fig. 3B). Note the difference in distribution between RILP and RILPsv when co-expressed with Rab7T22N; RILPsv dissociated from the membrane, whereas RILP remained associated to the membrane. This again suggests that RILP interacts more strongly with endogenous Rab7 than RILPsv.

Binding of RILPsv to Rab7 prolongs its GTP-bound active state

Fluorescent recovery after photobleaching (FRAP) was successfully used to study the GTPase activation cycle of EGFP-tagged Rab7 [1,28]. After bleaching a portion of membrane-bound EGFP-Rab7, the recovery of fluorescence in the bleached spot was measured in time by CLSM. The recovery represents GTP hydrolysis and replacement of bleached membrane-bound EGFP-Rab7 with fluorescent EGFP-Rab7 from the cytosol, and thus represents the Rab7 activation cycle. Using this approach we showed that RILP locks Rab7 in the active, membrane-bound form [1].

To determine whether RILPsv has a similar effect on the Rab7 cycle, RILP or RILPsv was expressed in a Mel JuSo cell line stably expressing EGFP-Rab7. As shown before, in wild type EGFP-Rab7 expressing cells the mobile fraction (the percentage of maximal recovered EGFP-Rab7) is 64% (Figs. 4A and B) [1,28]. RILP expressing cells showed rapid clustering of the EGFP-Rab7 containing vesicles and a concomitant drop in the mobile fraction of EGFP-Rab7 to approximately 10% (Figs. 4A and B). Expression of RILPsv had a similar effect on recovery; after bleaching, only 20% of the EGFP-Rab7 was recovered (Figs. 4A and B). In both cases an accurate recovery time ($t_{1/2}$) could not be determined.

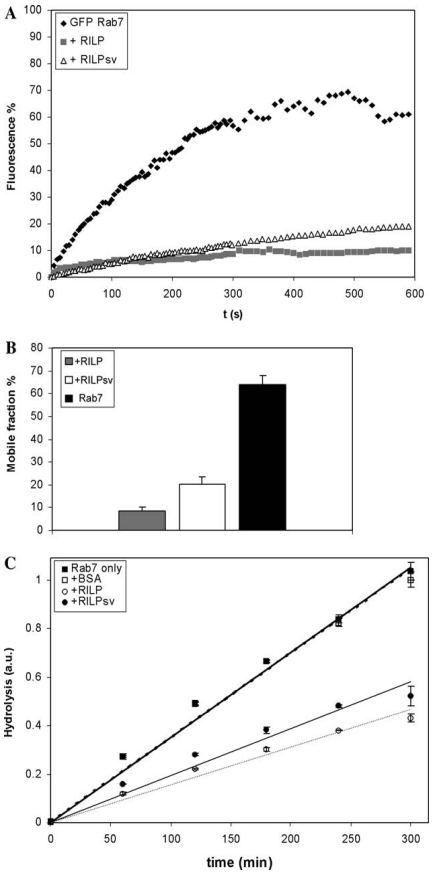

Fig. 4. RILPsv arrests Rab7 in the active state. (A) The Rab7 GTPase cycle was studied using FRAP. A portion of GFP-Rab7 compartments in control cells and cells expressing RILP or RILPsv were bleached and recovery of fluorescence in the bleached spot was plotted in a recovery curve. The fluorescence was related to the initial fluorescence set at 100%, $t = 0$ is the first measurement after the bleach. (B) Quantifications of the mobile fractions deduced from the recovery curves including SE are depicted ($n = 5$–10). (C) An in vitro assay was used to measure the GTPase cycle using [γ-^{32}P]GTP, in which the hydrolysis of GTP was followed in time by monitoring the release of [^{32}P]Pi. [^{32}P]Pi is slowly released from GTP-Rab7 (filled squares). Addition of His-RILP (open circles) and His-RILPsv (closed circles) significantly reduced the GTP hydrolysis rate of Rab7. BSA had no effect on the hydrolysis of Rab7 (open squares) and hydrolysis of Rab5 was not affected by the addition of His-RILP or His-RILPsv (data not shown).

Fig. 5. RILPsv fails to recruit dynein motors to late endocytic compartments. (A) CLSM analysis of Mel Juso cells ectopically expressing either RILP (upper panel) or RILPsv (middle and lower panels). RILP and RILPsv were labeled with anti-RILP (middle panels) and dynein–dynactin motors were visualized by anti-p150^{Glued} (left panels). (B) Motor recruitment in RILP and RILPsv expressing cells was quantified. Values are given as mean percentage of p150^{Glued} recruitment ± error bars indicating the standard deviation (>100 injected cells counted in two independent experiments). RILPsv shows a major reduction in dynein–dynactin motor recruitment. (C) Co-expression of RILP in RILPsv-expressing cells could restore the motor recruitment. RILP and RILPsv were expressed via micro-injection and labeled with anti-RILP (right panels) and dynein–dynactin motors were labeled by anti-p150^{Glued} (middle panels). Bars equal 10 μm.

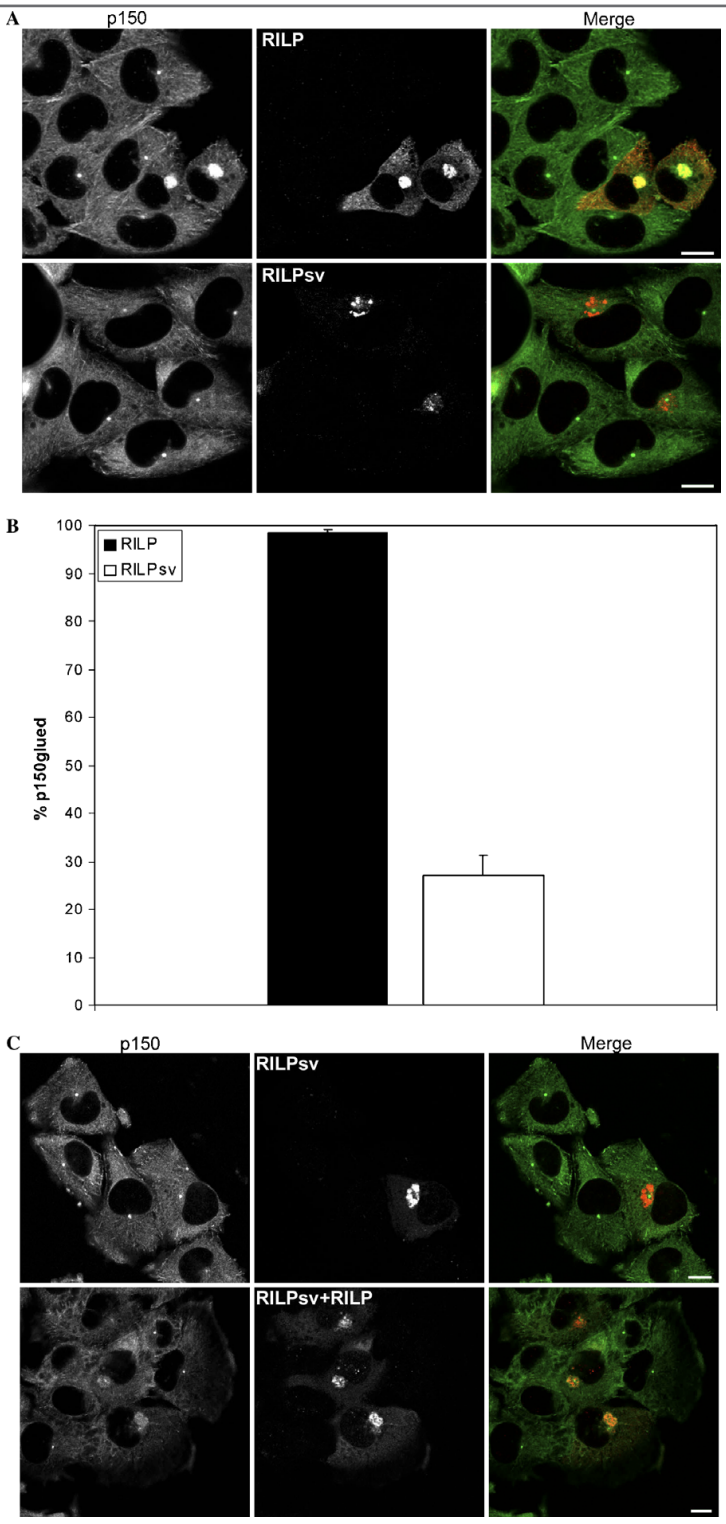
A
p150
Merge
RILP
RILPsv
B
RILP
RILPsv
% p150glued
100
90
80
70
60
50
40
30
20
10
0
C
p150
Merge
RILPsv
RILPsv+RILP

Beside the in vivo approach using FRAP, we used an in vitro approach using [γ-^{32}P]GTP to study the effect of His_6-RILP and His_6-RILPsv on the intrinsic GTPase activity of Rab7 [26,27]. Quantification of [^{32}P]Pi released from GTP-bound Rab7 showed that even after 5 h of hydrolysis saturation was not reached. This is consistent with the rather slow intrinsic GTPase activity of Rab7 [29] (Fig. 4C).

In order to test the effect of RILP and RILPsv on the hydrolysis rate of Rab7, His_6-RILP or His_6-RILPsv proteins were incubated with [γ-^{32}P]GTP loaded Rab7. Consistent with the FRAP data, addition of either His_6-RILP or His_6-RILPsv resulted in a significant decrease in GTP hydrolysis of Rab7 (Fig. 4C). Equimolar amounts of BSA had no effect on the GTP hydrolysis rate of Rab7 (Fig. 4C). Moreover, the addition of either His_6-RILP or His_6-RILPsv did not affect the hydrolysis rate of Rab5 (data not shown). Taken together, these data show that both RILP and RILPsv can strongly reduce Rab7 hydrolysis thereby keeping Rab7 in the active GTP-bound state.

Exon VII is critical for recruiting the minus-end dynein motor to late endocytic compartments

Although RILPsv like RILP interacts with Rab7, it results in a different phenotype upon ectopic expression. RILP has been shown to induce recruitment of the dynein–dynactin complex to late endosomal and lysosomal compartments [1]. To investigate whether RILPsv shares this ability with RILP, we injected cDNA encoding RILP or RILPsv in Mel Juso cells. After fixation, the p150^{Glued} subunit of the dynein–dynactin complex was detected. In RILP expressing cells, tight RILP-positive clusters were formed labeling for the p150^{Glued} subunit (Fig. 5A, upper panels). However, co-staining with p150^{Glued} was usually not observed in cells expressing RILPsv (Fig. 5A, lower panels). Quantification shows a significant decrease of approximately 70% in the recruitment of p150^{Glued} to the RILPsv-positive compartments (Fig. 5B). These findings indicate that exon VII is involved in the recruitment of the dynein–dynactin complex.

Interestingly, co-expression of RILP in RILPsv-expressing cells could restore motor recruitment (Fig. 5C), indicating that full-length RILP can compete with RILPsv for dynein recruitment to Rab7-positive compartments.

RILP and RILPsv both form hetero- and homo-dimers

Although RILPsv does not recruit the dynein–dynactin motor, it still induces clustering of late endocytic compartments. Other proteins have been described that cause clustering of late endosomal/lysosomal compartments independent of dynein–dynactin recruitment, such as mVPS18 and hVam6p [30,31]. These proteins are able to form homo-oligomers, which are critically involved in their ability to induce clustering. In addition, recent structural

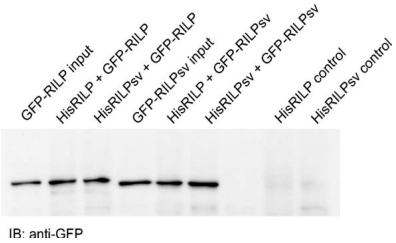

Fig. 6. RILP and RILPsv form hetero- and homo-dimers Mel Juso cells expressing GFP-RILP or GFP-RILPsv were lysed and incubated with either His-RILP or His-RILPsv coupled to Talon beads. Bound proteins were analyzed by immuno-blotting probed with anti-GFP antibodies. His-RILP and His-RILPsv can form both hetero- and homo-dimers with GFP-RILP and GFP-RILPsv. Non-transfected cells were used as a control.

data revealed that RILP acts as a dimer interacting with two Rab7 molecules [20]. To test the ability of RILP and RILPsv to form heterodimers, cells were electroporated with either EGFP-RILP or EGFP-RILPsv. Twenty-four hours after electroporation, cells were lysed and lysates were incubated with either His_6-RILP or His_6-RILPsv. Subsequently, lysates were run over a Ni^+ column to isolate the His-tagged proteins. Bound proteins were detected by Western blotting probed with anti-GFP (Fig. 6). His_6-RILP recruited both EGFP-RILP and EGFP-RILPsv. Moreover, His_6-RILPsv also interacted with EGFP-RILPsv. Thus, both RILP and RILPsv can form hetero- and homo-dimers, which might be responsible for the dynein-independent clustering of late endocytic structures in case of RILPsv.

Discussion

Late endosomal and lysosomal biogenesis is regulated by heterotypic and homotypic fusion, and bidirectional transport along microtubules to bring vesicles in close contact, for review see [4,6–8,32,33]. A key regulator in these processes is the small GTPase Rab7 [9–14]. Thus far, three Rab7 effectors have been described: Rabring7, RILP, and ORP1L [1,15–17]. All effectors induce lysosomal clustering. Additionally, ORP1L and RILP sequester dynein–dynactin motors onto lysosomal compartments resulting in a tight accumulation around the MTOC [1,17]. Here, we describe a natural occurring splice variant of RILP (RILPsv) lacking exon VII. Exon VII contains a proline-rich domain which is involved in protein–protein interactions. Like RILP, RILPsv also induces lysosomal clustering (albeit not as tight as RILP), but does not induce the recruitment of the dynein motor complex. This defines a proline-rich region of 27 amino acids, representing exon VII, involved in transferring a signal from Rab7 to the dynein motor complex.

Recently, Wang et al. [19] described two RILP-like proteins, RLP1 and RLP2, containing two highly conserved RILP homology domains. These proteins do not associate

with Rab7-positive compartments and do not affect the position of late endosomes and lysosomes. However, introduction of a 62 amino acid domain of RILP (274–333) could restore the ability of RLP1 to bind to Rab7 and to induce clustering of late endosomes and lysosomes.

RILPsv lacks amino acid 315–342, but still interacted with Rab7. This is in accordance with the observations by Wu et al. [20] that amino acids 241–320 of RILP are required for Rab7 binding, of which the main part is contained within RILPsv. Moreover, like RILP, RILPsv can lock Rab7 in the active, membrane-bound state as is shown by both the FRAP analyses and the GTPase assay. This is supported by the recently published crystal structure of Rab7 and RILP showing that RILP is a dimer surrounded by two GTP-loaded Rab7 proteins. The regions in RILP that contact the switch and interswitch regions of Rab7 are still present in RILPsv [20]. Interestingly, expression of RILPsv results in a different phenotype compared to that induced by RILP. This difference is more evident in HeLa cells, which have a less pronounced perinuclear localization of late endosomes and lysosomes compared to the melanoma-cell line Mel JuSo. We showed that the ability of RILPsv to induce recruitment of the minus-end dynein–dynactin motor complex is largely reduced, implicating exon VII in motor recruitment. Previously, we have shown that a deletion mutant of RILP lacking the N-terminal half (RILP-ΔN), still containing exon VII, fails to recruit the dynein motor as well [1]. Thus information in both the N-terminus and exon VII of RILP is required for dynein motor recruitment. Moreover, we show that RILP can compete with RILPsv for Rab7 binding, thereby inducing dynein motor recruitment. Thus, two products from the same gene can induce different effects in terms of motor protein recruitment, but compete for the same binding site: Rab7-GTP.

Although RILPsv cannot efficiently recruit the minus-end dynein motor, it induces late endosomal clustering. Two other late endosomal/lysosomal-associated proteins cause similar clustering without inducing dynein motor recruitment, mVPS18 and hvam6p [30,31]. These proteins are mammalian homologues of subunits of the yeast homotypic fusion complex, HOPS, which is involved in vacuolar fusion [34–42]. A common feature of mVPS18 and hvam6p is their CLH (clathrin homology) domain, which is essential for clustering of late endosomes and lysosomes. In addition, this domain appeared to be involved in homo-oligomerization and interaction with other components of the HOPS complex [30,31,43,44].

RILP has no CLH domain, but both RILP and RILPsv are able to hetero- and homo-dimerize. This might explain the observed phenotype for RILPsv. No dynein motor is recruited, but the hetero- or homo-dimerization of RILPsv with itself or endogenous RILP still results in clustering of lysosomal compartments, comparable to mVps18 and hvam6p. Yet, only full-length RILP induces dynein–dynactin motor recruitment resulting in a compact lysosomal cluster.

Our data describe a natural occurring splice variant of the Rab7 effector RILP lacking only 27 amino acids encoded in exon VII. This 27 amino acid, proline-rich stretch is critical for dynein-motor recruitment to Rab7-positive compartments and transport of these compartments to the microtubule minus-end. We show an example of a splice variant of an effector protein that adds an additional layer of complexity to the regulation of vesicle fusion and transport by Rab proteins.

Acknowledgments

We thank M. vd Vijver and D. Atsma for providing RNA isolated from different human tissues, members of the Neefixlab, A. Griekspoor and M. Voorhoeve for helpful discussions, and Lauran Oomen and Lenny Brocks for assistance with CLSM. This work was supported by grants from The Netherlands Cancer Society KWF and NWO (Zon MW PGS 912-03-026). N. Rocha is supported by a FCT/FSE PhD scholarship, within the Third Framework Program.

Appendix A. Supplementary data

Supplementary data associated with this article can be found, in the online version, at doi:10.1016/j.bbrc.2006.03.178.

References

[1] I. Jordens, M. Fernandez-Borja, M. Marsman, S. Dusseljee, L. Janssen, J. Calafat, H. Janssen, R. Wubbolts, J. Neefjes, The Rab7 effector protein RILP controls lysosomal transport by inducing the recruitment of dynein-dynactin motors, Curr. Biol. (2001) 1680–1685.
[2] E. Nielsen, F. Severin, J.M. Backer, A.A. Hyman, M. Zerial, Rab5 regulates motility of early endosomes on microtubules, Nat. Cell Biol. 1 (1999) 376–382.
[3] B. Short, C. Preisinger, J. Schaletzky, R. Kopajtich, F.A. Barr, The Rab6 GTPase regulates recruitment of the dynactin complex to Golgi membranes, Curr. Biol. 12 (2002) 1792–1795.
[4] I. Jordens, M. Marsman, C. Kuijl, J. Neefjes, Rab proteins, connecting transport and vesicle fusion, Traffic 6 (2005) 1070–1077.
[5] J.A. Hammer 3rd, X.S. Wu, Rabs grab motors: defining the connections between Rab GTPases and motor proteins, Curr. Opin. Cell Biol. 14 (2002) 69–75.
[6] M.C. Seabra, C. Wasmeier, Controlling the location and activation of Rab GTPases, Curr. Opin. Cell Biol. 16 (2004) 451–457.
[7] H. Stenmark, V.M. Olkkonen, The Rab GTPase family, Genome Biol. 2 (2001), REVIEWS3007.
[8] M. Zerial, H. McBride, Rab proteins as membrane organizers, Nat. Rev. Mol. Cell Biol. 2 (2001) 107–117.
[9] C. Bucci, P. Thomsen, P. Nicoziani, J. McCarthy, B. van Deurs, Rab7: a key to lysosome biogenesis, Mol. Biol. Cell 11 (2000) 467–480.
[10] Y. Feng, B. Press, A. Wandinger-Ness, Rab 7: an important regulator of late endocytic membrane traffic, J. Cell Biol. 131 (1995) 1435–1452.
[11] S. Meresse, J.P. Gorvel, P. Chavrier, The rab7 GTPase resides on a vesicular compartment connected to lysosomes, J. Cell Sci. 108 (Pt. 11) (1995) 3349–3358.
[12] B. Press, Y. Feng, B. Hoflack, A. Wandinger-Ness, Mutant Rab7 causes the accumulation of cathepsin D and cation-independent mannose 6-phosphate receptor in an early endocytic compartment, J. Cell Biol. 140 (1998) 1075–1089.

[13] F. Schimmoller, H. Riezman, Involvement of Ypt7p, a small GTPase, in traffic from late endosome to the vacuole in yeast, J. Cell Sci. 106 (Pt. 3) (1993) 823–830.
[14] H. Wichmann, L. Hengst, D. Gallwitz, Endocytosis in yeast: evidence for the involvement of a small GTP-binding protein (Ypt7p), Cell 71 (1992) 1131–1142.
[15] G. Cantalupo, P. Alifano, V. Roberti, C.B. Bruni, C. Bucci, Rab-interacting lysosomal protein (RILP): the Rab7 effector required for transport to lysosomes, EMBO J. 20 (2001) 683–693.
[16] K. Mizuno, A. Kitamura, T. Sasaki, Rabring7, a novel Rab7 target protein with a RING finger motif, Mol. Biol. Cell 14 (2003) 3741–3752.
[17] M. Johansson, M. Lehto, K. Tanhuanpaa, T.L. Cover, V.M. Olkkonen, The oxysterol-binding protein homologue ORP1L interacts with Rab7 and alters functional properties of late endocytic compartments, Mol. Biol. Cell 16 (2005) 5480–5492.
[18] T. Wang, W. Hong, Interorganellar regulation of lysosome positioning by the Golgi apparatus through Rab34 interaction with Rab-interacting lysosomal protein, Mol. Biol. Cell 13 (2002) 4317–4332.
[19] T. Wang, K.K. Wong, W. Hong, A unique region of RILP distinguishes it from its related proteins in its regulation of lysosomal morphology and interaction with Rab7 and Rab34, Mol. Biol. Cell 15 (2004) 815–826.
[20] M. Wu, T. Wang, E. Loh, W. Hong, H. Song, Structural basis for recruitment of RILP by small GTPase Rab7, EMBO J. 24 (2005) 1491–1501.
[21] S. Meresse, O. Steele-Mortimer, B.B. Finlay, J.P. Gorvel, The rab7 GTPase controls the maturation of Salmonella typhimurium-containing vacuoles in HeLa cells, EMBO J. 18 (1999) 4394–4403.
[22] H. Stenmark, R.G. Parton, O. Steele-Mortimer, A. Lutcke, J. Gruenberg, M. Zerial, Inhibition of rab5 GTPase activity stimulates membrane fusion in endocytosis, EMBO J. 13 (1994) 1287–1296.
[23] J.P. Gorvel, P. Chavrier, M. Zerial, J. Gruenberg, rab5 controls early endosome fusion in vitro, Cell 64 (1991) 915–925.
[24] C. Vennegoor, J. Calafat, P. Hageman, F. van Buitenen, H. Janssen, A. Kolk, P. Rumke, Biochemical characterization and cellular localization of a formalin-resistant melanoma-associated antigen reacting with monoclonal antibody NKI/C-3, Int. J. Cancer 35 (1985) 287–295.
[25] E.A. Reits, J.C. Vos, M. Gromme, J. Neefjes, The major substrates for TAP in vivo are derived from newly synthesized proteins, Nature 404 (2000) 774–778.
[26] D.R. Brandt, T. Asano, S.E. Pedersen, E.M. Ross, Reconstitution of catecholamine-stimulated guanosinetriphosphatase activity, Biochemistry 22 (1983) 4357–4362.
[27] T. Higashijima, K.M. Ferguson, P.C. Sternweis, E.M. Ross, M.D. Smigel, A.G. Gilman, The effect of activating ligands on the intrinsic fluorescence of guanine nucleotide-binding regulatory proteins, J. Biol. Chem. 262 (1987) 752–756.
[28] M. Marsman, I. Jordens, C. Kuijl, L. Janssen, J. Neefjes, Dynein-mediated vesicle transport controls intracellular Salmonella replication, Mol. Biol. Cell 15 (2004) 2954–2964.
[29] A.D. Shapiro, M.A. Riederer, S.R. Pfeffer, Biochemical analysis of rab9, a ras-like GTPase involved in protein transport from late endosomes to the trans Golgi network, J. Biol. Chem. 268 (1993) 6925–6931.
[30] S. Caplan, L.M. Hartnell, R.C. Aguilar, N. Naslavsky, J.S. Bonifacino, Human Vam6p promotes lysosome clustering and fusion in vivo, J. Cell Biol. 154 (2001) 109–122.
[31] V. Poupon, A. Stewart, S.R. Gray, R.C. Piper, J.P. Luzio, The role of mVps18p in clustering, fusion, and intracellular localization of late endocytic organelles, Mol. Biol. Cell 14 (2003) 4015–4027.
[32] P. Novick, M. Zerial, The diversity of Rab proteins in vesicle transport, Curr. Opin. Cell Biol. 9 (1997) 496–504.
[33] J. Somsel Rodman, A. Wandinger-Ness, Rab GTPases coordinate endocytosis, J. Cell Sci. 113 (Pt. 2) (2000) 183–192.
[34] M. Huizing, A. Didier, J. Walenta, Y. Anikster, W.A. Gahl, H. Kramer, Molecular cloning and characterization of human VPS18, VPS 11, VPS16, and VPS33, Gene 264 (2001) 241–247.
[35] B.Y. Kim, H. Kramer, A. Yamamoto, E. Kominami, S. Kohsaka, C. Akazawa, Molecular characterization of mammalian homologues of class C Vps proteins that interact with syntaxin-7, J. Biol. Chem. 276 (2001) 29393–29402.
[36] N. Nakamura, A. Hirata, Y. Ohsumi, Y. Wada, Vam2/Vps41p and Vam6/Vps39p are components of a protein complex on the vacuolar membranes and involved in the vacuolar assembly in the yeast Saccharomyces cerevisiae, J. Biol. Chem. 272 (1997) 11344–11349.
[37] A. Price, W. Wickner, C. Ungermann, Proteins needed for vesicle budding from the Golgi complex are also required for the docking step of homotypic vacuole fusion, J. Cell Biol. 148 (2000) 1223–1229.
[38] S.C. Richardson, S.C. Winistorfer, V. Poupon, J.P. Luzio, R.C. Piper, Mammalian late vacuole protein sorting orthologues participate in early endosomal fusion and interact with the cytoskeleton, Mol. Biol. Cell 15 (2004) 1197–1210.
[39] S.E. Rieder, S.D. Emr, A novel RING finger protein complex essential for a late step in protein transport to the yeast vacuole, Mol. Biol. Cell 8 (1997) 2307–2327.
[40] T.K. Sato, P. Rehling, M.R. Peterson, S.D. Emr, Class C Vps protein complex regulates vacuolar SNARE pairing and is required for vesicle docking/fusion, Mol. Cell 6 (2000) 661–671.
[41] D.F. Seals, G. Eitzen, N. Margolis, W.T. Wickner, A. Price, A Ypt/Rab effector complex containing the Sec1 homolog Vps33p is required for homotypic vacuole fusion, Proc. Natl. Acad. Sci. USA 97 (2000) 9402–9407.
[42] A.E. Wurmser, T.K. Sato, S.D. Emr, New component of the vacuolar class C-Vps complex couples nucleotide exchange on the Ypt7 GTPase to SNARE-dependent docking and fusion, J. Cell Biol. 151 (2000) 551–562.
[43] T. Darsow, D.J. Katzmann, C.R. Cowles, S.D. Emr, Vps41p function in the alkaline phosphatase pathway requires homo-oligomerization and interaction with AP-3 through two distinct domains, Mol. Biol. Cell 12 (2001) 37–51.
[44] J.A. Ybe, F.M. Brodsky, K. Hofmann, K. Lin, S.H. Liu, L. Chen, T.N. Earnest, R.J. Fletterick, P.K. Hwang, Clathrin self-assembly is mediated by a tandemly repeated superhelix, Nature 399 (1999) 371–375.